MASSIVE STAR FORMATION

ED CHURCHWELL
University of Wisconsin
475 N. Charter St.
Madison, WI 53706
USA

1. Introduction

One of the most durable problems in all of astrophysics is how stars are formed. Since the time of LaPlace astromomers have postulated numerous scenerios, but to the present this problem has resisted solution. This is especially true for massive stars. Massive star formation (MSF) has received much less observational and theoretical attention than low mass star formation and as a consequence much less is known about its physics, indeed it could be argued that we know too little to ask the right questions. Some, however, are obvious. For example, the mechanism(s) of cluster formation is still a mystery. In particular, what determines the IMF? What are the roles of fragmentation, differential galactic rotation, and turbulence in regulating the rate, and possibly the IMF, of star formation in molecular clouds? Are bipolar outflows the mechanism for shedding angular momentum from accretion disks? How does matter actually get from an accretion disk onto a protostar? Are massive stars formed entirely by accretion processes or a combination of accretion and stellar mergers? When are stellar winds established, what is their relationship to bipolar outflows, and what role do they play in the formation process?

A few things are known. For example, massive stars typically, perhaps always, form in conjunction with an associated cluster of lower mass stars. They form in massive molecular cloud cores which are generally heavily obscured at optical and UV wavelengths. Consequently, they generally can only be observed at infrared and radio wavelengths. The velocity, density, and tempurature structure of the circumstellar matter around a forming massive star is expected to change by orders of magnitude over distances of $<$1000 AU. Although, little is known about the detailed distribution and kinematics of gas and dust at distances within several hundred AU of forming massive stars nor the physical process by which they form, there are some critical size scales that we can approximately identify from present observations and theoretical considerations. Stellar winds are expected to accompany MSF with wind velocities up to a few thousand km/s, the effects of which may be detectable out to 1000 AU from the protostar in a hot wind-shocked cavity which supports observed shell-like and cometary ultracompact (UC HII) regions. Dense and massive molecular outflows extending out to several pcs are presumably driven by a central massive protostar. Although the mechanism for initiating and driving these outflows is still unknown, ample observational evidence confirms their existence. Ultracompact HII regions surround young massive stars out to radii of about 10^{17} cm typically. See Churchwell (1990, 1991, 1995, 1997a) for reviews of the properties of UC HII regions. During formation, it is expected that a massive accretion disk forms which feeds the central protostar from infalling ambient cloud core material; these disks, if they exist, may have radii of a hundred AU or more and masses containing a significant fraction of the central protostar mass. The protostar itself may have a diameter of 10^{12} cm or more depending on the stage of evolution.

I will review some of the established properties of MSF regions in §2. The morphologies, ages, and dynamics of UCHII regions will be discussed in §3. §4 summarizes a recent determination of the angular expansion rate of G5.89 and in §5 dust emission from UC HII regions is discussed. The properties of hot, molecular, cloud cores where massive stars are formed are addressed in §6. A summary is given of the recently discovered hard X-ray emission from W3 in §7. The properties and implications of molecular outflows associated with MSF are examined in §8 and a brief summary is given in §9.

2. TYPICAL PROPERTIES OF MSF REGIONS

MSF occurs in the cores of massive molecular clouds. These cloud cores generally have very large optical extinctions (>50 mag), kinetic temperatures 50-200 K, and densities 10^5 - 10^7 cm^{-3}. These molecular cores are rich chemical laboratories in which many molecular species have been detected and from which much information on the physical conditions have been inferred (see §6). Radio continuum images often show multiple components indicating the presence of several hot, young stars. In fact, massive stars always seem to be accompanied by a cluster of lower mass stars. Within a given region of space, star formation is often (perhaps always) not coeval; a very good example of this is the G9.62+0.19 complex (Hofner *et al.* 1995) in which four separate epochs of massive star formation are apparent. Sign

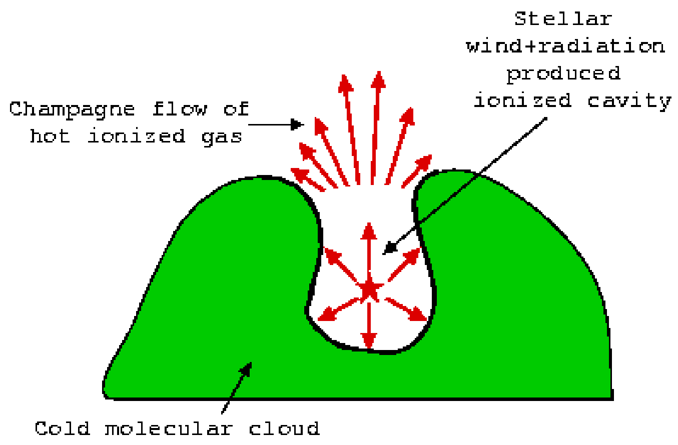

Figure 1. A schematic illustrating a champagne flow produced by a newly formed hot star whose wind and radiation evacuates a hot, ionized cavity at the edge of a large molecular cloud. At the cloud boundary, the ionized cavity "breaks out" and one sees a flow of ionized gas in directions where the gas is unimpeded by the molecular cloud. The flow is produced by a pressure gradient because of the over-pressure in the HII cavity relative to the ambient ISM pressure.

posts of massive star formation are UC HII regions, water masers, methanol masers, and luminous far infrared emission with colors in the range initially defined by Wood & Churchwell (1989b) and subsequently refined by others. The infrared flux distributions typically peak at about 100 μm and the typical dust temperatures are about 30 K, but of course the dust temperatures are a function of distance from the central YSO. The UC HII regions formed by massive YSOs have electron densities of $\sim 10^5$ cm^{-3}, emission measures of $\sim 10^8$ pc cm^{-6}, and diameters of a few times 10^{16} cm.

Massive stars are tightly confined to the Galactic plane (Wood & Churchwell 1989b; White, Becker, & Helfand 1991; Helfand, Zoonematkermani, Becker, & White 1992; Becker, White, Helfand, & Zoonematkermani 1994) There is some controversy over the exact value of the Z-scale height, but everyone agrees that it is $\leq$0.8 degrees.

3. MORPHOLOGIES, AGES, AND DYNAMICS OF UC HII REGIONS

UC HII regions have a surprisingly small range of morphologies which Wood & Churchwell (1989a; hereafter WC89a) classified as: cometary; core-halo; shell-like; irregular or multiply peaked; and spherical or unresolved. WC89a also pointed out that there are far too many UC HII regions to be consistent with classical Strömgren theory and concluded that UC HII regions must remain in a compact state $\sim 10^5$ yr, a factor of a hundred or so longer than the nebular sound crossing time. In fact, the morphology of a UC HII region is a complicated function of its age, the dynamics of both H^+ and H_2 gas, the density structure of the local ambient ISM, and the motion of the HII region relative to the ambient medium. Because the morphology of a UC HII region depends on so many factors, it has not been as easy as one might have supposed to isolate the primary mechanism that determines the morphology and maintains UC HII regions in a compact state. In this section, I will review the mechanisms proposed to explain the morphologies and lifetimes of UC HII regions.

3.1. CHAMPAGNE FLOW OR "BLISTER MODELS"

These models have their origin in the 1970s when it was believed that massive stars form preferentially near the boundaries of molecular clouds and as the stars become self-luminous they ionize a cavity at the surface of the cloud. The ionized cavity is confined in directions where the stellar photons are intercepted by the molecular cloud but ionized gas freely flows away from the cavity in directions away from the molecular cloud. This class of models produce cometary morphologies and are illustrated schematically in Figure 1. Further references to and variants of this class of models can be found in York, Tenorio-Tagle, & Bodenheimer (1983) and references therein. Garay, Lizano, & Gomez (1994) incorporated the effects of stellar winds and Forster *et al.* (1990) and Fey *et al.* (1995) and others have shown that star formation in a medium with a steep density gradient will also produce cometary morphologies. This class of models, however, has the basic problem that they evolve on a dynamical time scale and are therefore unlikely to be able to account for ages a factor of 10-100 times greater, as required by the large number of observed UC HII regions. There are several cases where this model seems applicable (e.g. Mon R2, Massi, Felli, & Simon 1985). Certainly, in situations where an embedded O-star is emerging from its natal molecular cloud, the champagne flow will apply.

3.2. IN-FALL MODELS

Reid *et al.* (1981), Zheng *et al.* (1985), Ho & Haschick (1986), Keto, Ho, & Reid (1987); and Keto, Ho, & Haschick (1987; 1988) proposed that UC HII regions can be maintained in a compact state well in excess of their sound crossing times (i.e. dynamical ages) due to gravitational in-fall of molecular gas. This is illustrated schematically in Figure 2. Although this class of models might possibly account for the ages of UC HII regions, it is not clear how they can account for UC HII morphologies. Also, the required

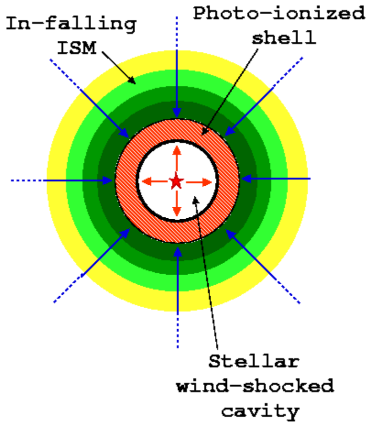

Figure 2. A schematic illustrating confinement of a UC HII region by in-falling ambient molecular gas. The in-falling molecular gas provides both an increase in density and pressure at the I-front of the UC HII region.

in-fall rates have not been worked out so it is not clear if typical cloud cores can actually supply them over the required $\sim 10^5$ yr timescale.

3.3. PHOTO-EVAPORATING DISK MODEL

This model, developed by Hollenbach *et al.* (1993, 1994) uses the expected presence of a massive accretion disk and the strong UV radiation field of a massive YSO to explain the longevity of UC HII regions. The idea is basically that the UV radiation from the central star ionizes the outer envelope of the accretion disk. Inside the radius r_g, the photoevaporated gas flows away from the disk and forms a compact HII region which is continuously replenished as long as the accretion disk persists. Outside the radius r_g, the gas flows away from the disk at speeds greater than the escape velocity and produces a wind from the disk. In cases where the star has a strong stellar wind, the radius at which the disk wind occurs is greater than r_g due to stellar wind pressure. This is shown schematically in Figure 3 (Fig. 1 of Hollenbach *et al.* 1993). Although this picture gives a natural explanation for the longevity of UC HII regions in terms of properties that we believe are integral to such regions, it does not address the observed variety of morphologies. It may very well be applicable to those compact nebulae that are unresolved by the VLA as suggested by Hollenbach *et al.* (1993, 1994).

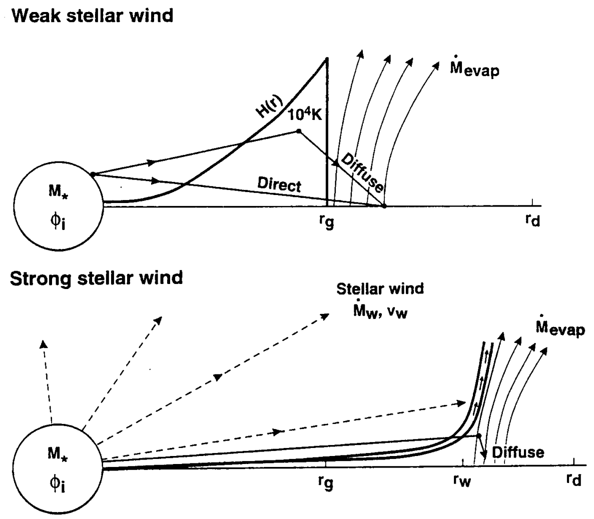

Figure 3. A schematic illustrating the photoevaporation of a disk around a massive star. The upper panel illustrates the weak stellar wind case where both direct stellar and diffuse photons ionize the disk. Beyond the radius r_g the ionized photons escape to form a compact HII region around the star. The lower panel illustrates the strong wind case where the region of escaping ionized gas is pushed further from the central star by the stronger stellar wind. These illustrations are from Hollenbach, Johnstone, & Shu (1993).

3.4. PRESSURE CONFINED UC HII REGIONS

In recent years it has been discovered that the molecular density in the immediate vicinity of UC HII regions is much higher than originally thought, in several cases as high as 10^7 cm^{-3}. DePree, Rodriguez, & Goss (1995) and DePree, Goss, & Gaum (1998) have postulated that at such densities, the ambient medium around UC HII regions can provide enough pressure to confine an HII region for periods up to 10^5 years as required. This idea is shown schematically in Figure 4. Xie *et al.* (1996) have suggested an alternative version of this idea. They suggest that turbulent pressure could provide the high ambient pressures needed for confinement. In this case, because the pressure does not necessarily arise from particularly high densities, it avoids the high emission measures (EM$\geq 10^{10}$ pc cm^{-6}) predicted by the DePree *et al.* picture. Although confinement by external pressure (gas or turbulent) may be able to explain the longevities of UC HII regions, it does not address their morphologies. Also, it is unclear if the required high densities are extensive enough to provide confinement for the required time.

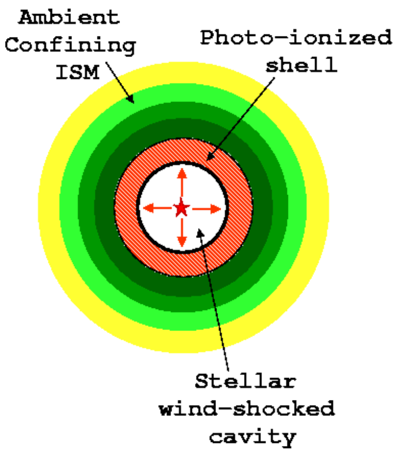

Figure 4. A schematic illustrating the confinement of a UC HII region by dense, ambient, molecular gas which provides the thermal pressure required for confinement. The sketch implies that the density rises toward the I-front of the HII region, as suggested by observations.

3.5. STELLAR WIND SUPPORTED BOW SHOCK MODEL

Wood & Churchwell (1989a) suggested that the cometary UC HII regions could be produced by a stellar wind supported bow shock. MacLow *et al.* (1991), and VanBuren *et al.* (1990) have calculated bow shock models which satisfactorily reproduce both cometary and core-halo morphologies. The idea here is that the YSO has a small velocity relative to the natal molecular cloud core (simply due to the velocity dispersion of the OB association to which the YSO belongs). This relative motion causes a bow shock due to ram pressure of the ambient medium in the direction of motion. This is opposed by the pressure produced by the stellar wind which shocks a low density, but very hot cavity inside the observed HII shell. This hypothesis provides a static configuration for the UC HII region which is neither expanding nor contracting and will remain in this state as long as the YSO remains in the molecular cloud. In this picture, a cometary morphology is observed when viewed "from the side" and a core-halo morphology is observed when viewed "head-on" or "tail-on". It also follows that spherical and shell-like morphologies can prevail when the YSO has little or no motion relative to the ambient medium, and in this case, the nebula would probably be expanding rather than in a static state. This scenerio is shown schematically in Figure 5. It has been questioned by several groups either because the velocity structure does not seem to follow model predictions (Lumsden & Hoare 1996) or because the model calculated by Van Buren *et al.* (1990) required a relatively high velocity so the dwell time in the natal

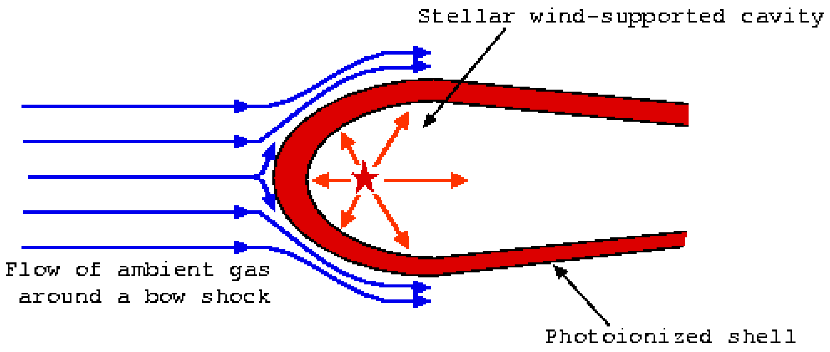

Figure 5. A schematic illustrating the confinement of a UC HII region by a bow shock produced by ambient molecular gas flowing past a newly formed massive star. The ionized shell is supported from inside by the stellar wind-shocked cavity. The assumption here is that the star is moving supersonically relative to the ambient natal molecular cloud (> a few tenths of a km/s).

molecular core would be too short. Neither of these may be fatal as there are counter arguments to both criticisms.

3.6. MASS-LOADED STELLAR WINDS

Dyson, Williams, & Redman (1995), Williams, Dyson, & Redman (1996), Dyson (1994), Redman, Williams, & Dyson (1996), and Lizano *et al.* (1996) proposed that UC HII regions can be maintained in a compact state via mass loaded stellar winds. The idea is that when the medium surrounding a massive young star contains many small, dense, and neutral condensations, the stellar wind plus UV radiation will ablate and photoionize the envelopes of the condensations, thereby continuously replenishing the nebular gas and producing small cometary structures like those observed in the Orion Nebula by O'Dell and coworkers. The continuous release of newly ionized gas into the nebula via photoionization of the embedded condensations traps the I-front and maintains the nebula in a compact state. This is illustrated in Figure 6 which is similar to a figure in Lizano *et al.* (1996). This model addresses the longevity of UC HII regions, but does not explain their morphologies.

Which model is correct? Possibly all the above may be valid in certain nebulae at particular evolutionary stages. The bow shock model is compelling because it can explain three of the observed morphological types and the lifetime problem, but it may not be the only explanation. For example, when a star exits its natal cloud, it should produce a champagne flow. It is possible to test the various hypotheses by obtaining high reso-

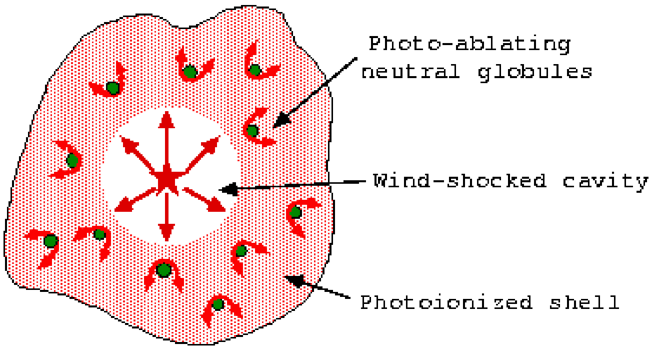

Figure 6. A schematic illustrating confinement of a UC HII region by mass loading the nebula from embedded molecular globules which are slowly photoevaporated and thereby continuously replenish the ionized gas maintaining the HII region in a dense, compact state.

lution velocity distributions of the ionized gas (via recombination lines or infrared fine structure lines) since each of the models predict rather different kinematics of the ionized gas. At present, such information does not exist for most nebulae.

4. THE ANGULAR EXPANSION RATE OF G5.89-0.39

In a effort to test some of the ideas proposed in §3, Acord, Churchwell, & Wood (1998; hereafter ACW98) used the VLA at three epochs over a period of 5.3 years to determine the angular expansion rates of G5.89-0.39 (shell-like) and G34.26+0.15 (cometary). Both of these UC HII regions are good candidates for measuring their angular expansion rates because they are among the brightest UC HII regions known at radio wavelengths and have approximately symmetric morphologies. G5.89-0.39 has an approximately spherical geometry which simplifies interpretation of its angular motions. Two independent techniques were used: 1) by scaling an earlier epoch image until it coincides with that of a later epoch image; and, 2) by differencing images obtained at two different epochs using the "cross-calibration" technique developed by Masson (1986, 1989). ACW98 found an expansion rate of 4 ± 1 mas yr^{-1}. From an analysis of the H42α line, ACW98 further inferred a radial expansion velocity of $v_{exp} \sim 35$ km s^{-1} under the assumption that random turbulent motions are no more than twice the thermal motions (i.e. turbulent FWHM$\leq$ 30 km s^{-1}). With an estimate of the expansion velocity of the nebula, they derived the distance to the nebula from the relation $D = v_{exp}/\mu$ where μ is the angular expansion rate. ACW98 find $D = 2.0^{+0.7}_{-0.4}$ kpc. The kinematic distance of this source is in the range 2.5 to 3.0 kpc, but at galactic longitudes $< 6^0$, kinematic distances are quite uncertain. For an expansion velocity of $\sim$35 km s^{-1} and an angular radius of the bright shell of 0.010$\pm$0.002 pc, ACW98 infer a dynamical age of only 600^{+250}_{-125} yr, making this one of the youngest nebulae known. The fact that this nebula is expanding does not eliminate the bow shock model as this source has a spherical shell morphology which implies that it has little or no motion relative to the local ISM and therefore it is not confined by a bow shock. The program to obtain angular expansion rates is continuing.

5. DUST ASSOCIATED WITH UC HII REGIONS

MSF regions are among the brightest objects in the Galaxy in the far infrared. The reason for this is that massive YSOs are very luminous and deeply embedded in natal molecular gas and dust clouds. The dust ultimately absorbs all the radiation from all the stars in the cluster and reradiates it as infrared radiation at wavelengths determined by the temperature of the dust. At increasing distances from a UC HII region the dust temperatures decrease. The dust at greater radii radiate at ever longer IR wavelengths. At wavelengths shorter than about 3mm thermal dust emission dominates free-free emission from the gas. Because the dust has a temperature gradient with radius, the SED is broader than a single temperature Planck function. The SED of a typical MSF region is shown schematically in Figure 7 from radio wavelengths to the near infrared. The radiation mechanisms and properties of each region of the SED are indicated in Figure 7. The peak IR flux is a factor of 10^3 to 10^6 greater than that of the optically thin radio free-free emission. The radio flux density is a measure of the stellar ionizing flux and the FIR emission is a measure of the total radiation over all wavelengths from all stars in the cluster. Kurtz, Churchwell, & Wood (1994) showed that the value of the FIR to radio flux ratio is a function of the spectral type of the star responsible for ionization of the nebula; in the log the ratio is $\sim$6 for a B3 star and $\sim$3 for an O4 star. They also showed that MSF regions with a given 100μ flux to 2cm flux density essentially always have a larger total luminosity than can be produced by a single hot star of that luminosity. From this, they argued that MSF is always accompanied by a cluster of stars. This seems to be born out by observations as all MSF regions which have been imaged in the near infrared show an associated cluster of stars.

The IR SEDs of MSF regions have been modeled by several groups including Krügel&Mezger (1975); Leung (1976); Tielens&de Jong (1979); Tutukov&Shustov (1981); Lee&Draine (1985); Chini, Krügel, &Kreysa (1986); Hoare *et al.* (1988); Churchwell, Wolfire, & Wood (1990; hereafter CWW);

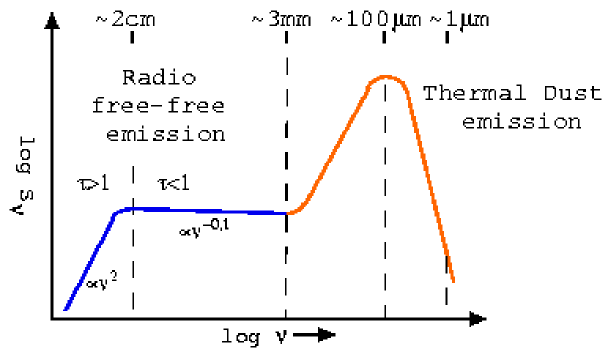

Figure 7. A schematic of the spectral energy distribution of a UC HII region from radio to the near infrared. S_ν is the flux density and ν is the frequency. Several key wavelengths are indicated along the top of the figure.

Wolfire & Churchwell (1994); and Faison *et al.* (1998). The latter three papers included a range of dust sizes at each position. In all models, spherical symmetry and a Planck function for the input stellar spectrum were assumed. The multi-source models of Faison *et al.* (1998) give an overview of the predicted range of dust properties associated with MSF regions heated by stars of type O5 to B0. In all cases, a central dust free cavity is required to fit the observed SEDs. No significant amounts of dust can exist close to the star(s) because they would produce too much NIR emission. The dust free cavities are typically about a factor of ten larger than the dust sublimation radius, thus the inner radius of the dust shell is determined not by photodestruction but probably by radiation pressure and/or stellar winds. The outer radii of the dust shell, defined by the radius at which the dust can no longer be distinguished from the ambient dust, are very large ranging from ~1 to ~4 pc. The ratio of outer to inner dust shell radii are in the range ~50 to ~150. The large outer radii are required in order to have dust cool enough that they emit most of their radiation at ~100 μm. The dust temperatures drop very sharply in the inner 20% of the dust shell radius, then decrease more slowly (as expected for an optically thin spherically symmetric cloud) in the outer 80% of the shell (see CWW90). The average dust temperatures at the inner dust shell boundary are 340 K to 200 K, depending on the region, and ~20 K at the outer boundary. Constant density models fit the data better than power-law density gradients.

The 9.7 μm silicate feature is often strong and always in absorption with spatial resolutions used so far (see Faison *et al.* 1998; Roelfsema *et al.* 1996). Polycyclic aromatic hydrocarbon features in the range 3 to 12 μm are often detected toward MSF regions and in some cases are the dominant features in this wavelength range (Roelfsema *et al.* 1996).

6. HOT MOLECULAR CLOUD CORES

What about the nature of the natal molecular cloud cores in which massive star formation occurs? Considerable work has been done on these regions by many groups in the past few years. I will try to summarize some of the main results of the past few years. It will be impossible to reference all the work done in this area and I apologize to those whose work I do not quote. I will not discuss molecular abundances, chemistry, grain mantle destruction and its impact on gas phase abundances, nor freezing out of gas phase molecules onto grains as these topics will be covered by other speakers. Molecular cloud cores where massive stars form are hot, dense, compact, and dynamic. Their temperature and density decrease with distance from the center and the enclosed mass increases. Cesaroni *et al.* (1991, 1992), Churchwell, Walmsley, & Wood (1992), Hofner *et al.* (1995) and others have measured hot core properties toward a number of MSF regions. Using $C^{34}S$ (2-1; 3-2; and 5-4) and NH_3 (1,1; 2,2; 4,4; and 5,5) Cesaroni *et al.* (1991, 1992) showed that typical hot cores have densities $\sim 10^6$ cm^{-3}; temperatures ~100-200 K; mass ~1000 $M_\odot$, and diameters ~0.5 pc. A particular example is the MSF core in which G9.62 is embedded. Hofner *et al.* (1995) has observed this region in several molecular line probes as well as radio continuum emission. From a $C^{18}O$ (1-0) image obtained at OVRO, they find a core of extent 0.6x0.3 pc, mass ~1000 $M_\odot$, average hydrogen density $2\text{x}10^5$ cm^{-3}, and average temperature over the entire core $\geq$30 K. Embedded in this core are two very young B stars (components D and E) which have formed very dense and compact UC HII regions and a currently forming massive protostar in a rapid stage of accretion (component F) all aligned along a SE-NW ridge. In addition, a string of H_2O, OH, CH_3OH, and NH_3 (5,5) masers are found along the central ridge between the D and E UC HII regions. This is illustrated in Figure 8 which shows the molecular core by contours, the radio continuum emission in grey scale, and the various masers by different symbols. This is the only object in the sky where the NH_3 (5,5) maser has been detected. It is located close to component E. This region also illustrates another morphological feature that seems fairly common in MSF regions, namely, the tendency for masers and star formation to occur along linear features. In a high resolution study of H_2O masers, Hofner & Churchwell (1996) noted that water masers often occur in linear features possibly indicating the tendency of cloud cores to form disk-like morphologies (Cesaroni *et al.* 1998), as discussed below. Finally, the G9.62 region appears to show at least four different epochs of massive star formation implied by the diameters and mean densities of HII regions

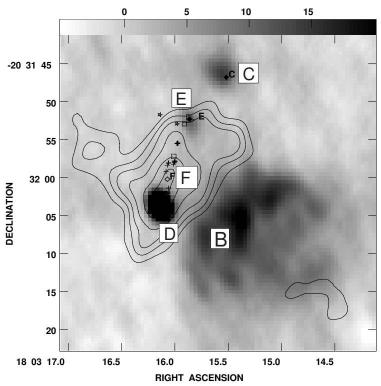

Figure 8. The $C^{18}O$ (1-0) core toward the massive star formation complex known as G9.62. The CO core is indicated by contours. The gray scale is the radio free- free emission produced by ionized Hydrogen. Discrete radio continuum sources are designated as components B, C, D, E, and F. The youngest and densest components D, E, and F are all embedded in the $C^{18}O$ core. There are also numerous water, ammonia, methanol, and hydroxyl masers located along a ridge running along the major axis of the CO core. See the caption for figure 3 in Hofner et al. (1995) for a definition of the various symbols. There are HII regions with a range of sizes and densities in this complex which Hofner et al. (1995) have argued indicate a range of ages. This figure is from Hofner et al. (1995).

A (oldest); B (intermediate age); C, D, and E (just emerging HII regions); and F (a protostar).

Cesaroni *et al.* (1994) pointed out an apparent luminosity paradox toward MSF cores. They found that the luminosities obtained by assuming that the cores are spherical, constant temperature blackbodies with temperatures and diameters derived from molecular line observations were about 5 times those obtained from integrated IRAS fluxes. The blackbody luminosities were calculated using the temperatures obtained from NH_3 line ratios (or excitation models) and diameters measured from the half-power distributions of the the NH_3 emission. This apparent paradox was resolved by Cesaroni *et al.* (1998) who measured the temperature profiles toward three MSF cores and modeled their temperature profiles using spherical and disk-like geometries. They found in all three cases that disk-like geometries reproduced the observed profiles quite accurately, but spherical models did not. This is illustrated in Figure 9 taken from Cesaroni *et al.* (1998). Further, cores with the observed temperature gradients and disk-like geometries have luminosities in agreement with those derived from the IRAS fluxes. The tendency of star-forming cloud cores to evolve to disk-like geometries may be the reason why masers and star formation often seem to occur in “elongated filaments”.

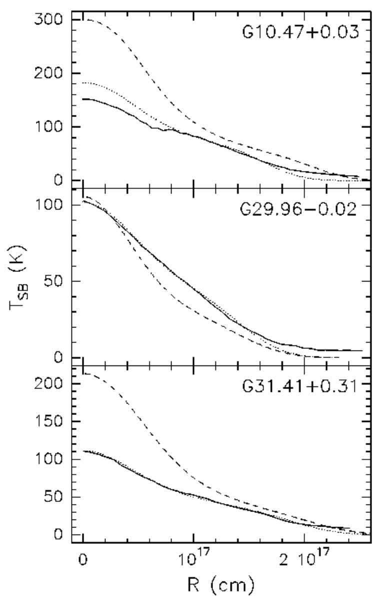

Figure 9. A comparison of model temperature profiles with observationally determined temperature distributions of three hot cores from Cesaroni *et al.* (1998). The dashed curves are for best fit spherical geometries, the solid curves are the observed temperatures, and the dotted curves are for disk-like geometries. See Cesaroni *et al.* (1998) for the input parameters and model results. The main point these models emphasize is that a disk-like geometry produces far better fits to the observed temperature profiles than a spherical geometry in all three sources.

7. HARD X-RAY EMISSION FROM MSF REGIONS

Main sequence OB stars and evolved stars are X-ray emitters. It has been postulated that this emission is produced either in a hot corona at the base of a stellar wind (Cassinelli&Olson 1979) and/or by shocks throughout the stellar wind (Lucy 1982). This emission generally occurs at energies $\leq$4 kev. X-rays have been observed in a small number of star forming regions such as ρOph and the Orion Nebula (Koyama *et al.* 1992; Yamauchi and Koyama 1993a). In both regions many of the X-ray sources have been identified with low-mass premain-sequence (PMS) stars. A further very intriguing result is the discovery of FeXXV line emission at 6.7 kev whose distribution is tightly confined to the disk of the Galaxy (Yamauchi and Koyama 1993b), similar to that of CO and O stars. Gas that can produce this line requires a temperature $\geq 70\text{x}10^6$ K and it is very difficult to understand how it can be so tightly confined to the Galactic disk. Motivated by the detection of X-ray emission from low-mass PMS stars and the discovery of the disk component of FeXXV line emission, Hofner & Churchwell (1997; hereafter HC97) used

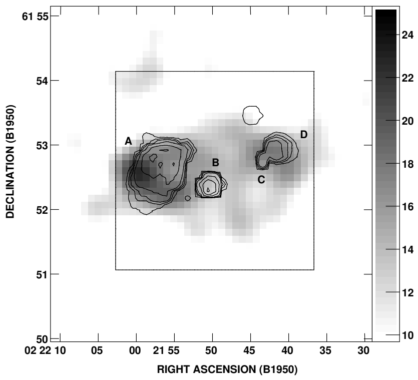

Figure 10. A comparison of radio continuum emission at 8.3 GHz from Adler, Wood, & Goss (1996) (contours) with X-ray emission in the energy range 0.5-10 kev (gray scale) toward the W3 complex. This is Fig. 1 from HC97 and it shows that the most intense hard X-ray emission coincides well with the UC HII regions in this complex.

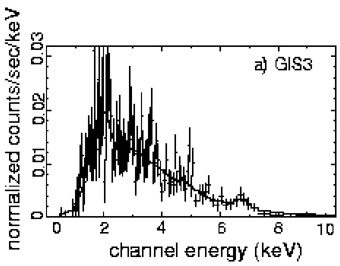

Figure 11. The observed X-ray spectrum integrated over a 6' diameter toward the core of W3 obtained with the GIS3 spectrometer on the ASCA satellite. The FeXXV line at ~6.7 kev is apparent in this spectrum. From HC97.

the ASCA satellite to search for X-ray emission from the MSF region W3. Their rationale was that massive protostars have fast and massive winds which are thought to produce a very hot ($\sim 10^8$ K), shocked cavity that supports the observed UC HII shell. This cavity should emit rather hard X-rays and possibly provide an explanation for how the FeXXV line can be so tightly confined to the Galactic disk, as O stars are also tightly confined to the disk. HC97 detected X-ray emission coincident with the UC HII regions which define the core of the W3 MSF region. The distribution of X-ray emission in the energy range 0.5-10 kev toward W3 is shown in Figure 10.

The X-ray spectrum toward the W3 core is shown in Figure 11. The X-ray flux is maximum at $\sim$2 kev but emission is seen as high as $\sim$8 kev. The FeXXV line at 6.7 kev, shown in Fig. 11, has a flux of $\sim 1.2 \times 10^{-5}$ photons $cm^{-2}\ s^{-1}$. A Raymond & Smith (1977) model fit to the observed spectrum, including extinction by interstellar hydrogen, implies the following properties of the emitting gas: T$\sim 7 \times 10^{7}$ K; a volume emission measure of 2.1×10^{56} cm^{-3}; an X-ray flux in the 2-10 kev range of 2.6×10^{-12} erg $cm^{-2}\ s^{-1}$; and a luminosity of $\sim 2 \times 10^{33}$ ergs s^{-1} in the 2-10 kev energy range. An absorbing hydrogen column density of 2.1×10^{22} cm^{-2} is inferred by the model, which is consistent with that measured by Dickel, Goss, & Condon (1996).

What is the origin of the observed hard X-ray emission in W3? The stellar coronal emission and shocks within stellar winds do not appear to be energetic enough to produce the emission above a few kev and there are probably not enough low-mass PMS stars to produce the observed flux from W3. The X-ray emission from W3 is a factor of 30 to 3000 times higher than Orion and ρ Oph, respectively. Thus, if low-mass PMS stars provide the X-ray emission, W3 would have to contain a substantially larger number of such stars than either Orion or ρ Oph. PMS stars also do not produce FeXXV line emission, so another explanation for this would be required. HC97 suggested that the wind shocked cavity associated with UC HII regions would provide a natural explain for both the presence of the FeXXV line and its confinement to the Galactic plane. However, this does not explain the apparent extended X-ray component toward the W3 complex. If the stenght of the FeXXV line from W3 is typical of MSF regions, then it does not appear that UC HII regions could be the major contributor to the disk component of FeXXV emission. However, only one such region has been observed so far, and it could well be that W3 is under-luminous relative to other such regions. More MSF regions need to be observed in the 1-10 kev energy range to resolve this issue.

8. MOLECULAR OUTFLOWS ASSOCIATED WITH MSF

8.1. THE FREQUENCY OF OUTFLOWS FROM MSF REGIONS

By 1995 several MSF regions had been observed to have molecular outflows. Among these were the Orion IRc2 outflow (Kwan & Scoville 1976; Zuckerman, Kuiper, & Rodriguez Kuiper 1976; Downes *et al.* 1981; Erickson *et al.* 1982; Wright *et al.* 1983; Allen & Burton 1993, and others); G5.89 (Harvey & Forveille 1988; Cesaroni *et al.* 1991; Choi, Evans, & Jaffe 1993); DR21 (Garden *et al.* 1991a,b; Garden & Carlstrom 1992); NGC 6334I (Bachiller & Cernicharo 1990); G34.26 and G10.62 (Cesaroni *et al.* 1991); W75N (Hunter *et al.* 1994); W3IRS 5, GL490, GL2591, S140, and CephA (Choi, Evans, & Jaffe 1993); and several low-mass and high-mass outflows are reported by Cabrit & Bertout (1992) and Lada (1985). In an effort to better determine the frequency of molecular outflows in MSF regions, Shepherd & Churchwell (1995; hereafter SC95) observed and analyzed the CO(1-0) line profiles with high signal-to-noise toward 94 UC HII regions (HPBW$\sim$60"). They found that fully 90% of this sample had line wing emission in excess of a gaussian profile fit to the core of the line. These results indicate gas motions in excess of thermal plus turbulent motions, but they do not necessarily indicate bipolar outflows as rotation, or expansion, or contraction, or different velocity components along the ling of sight could also produce excess line wings. To determine if the excess line wings are due to outflows Shepherd & Churchwell (1996; hereafter SC96) mapped a selection of 10 of the sources observed to have excess line wings by SC95. They found five to have well defined outflows, two had multiple velocity components along the line of sight and were not outflows, and three had either S/N ratios that were too low to confidently map or weak CO emission was in the reference position such that the images were unusable. They conclude that at least 50%, and possibly as high as 80%, of the selected sample have bipolar outflows.

8.2. MOLECULAR BIPOLAR OUTFLOW PROPERTIES

In Table 1, I have tabulated the sources toward which massive outflows have been detected. These are listed in order of increasing RA. Along with the source names and their positions, I also give the distances from the Sun D, the HII luminosities L_{HII} as determined from radio free-free flux densities or as given by the reference in Table 2, and the total luminosity of the HII region and associated cluster L_{IR} as determined from the integrated infrared flux. The distances are taken from the references listed in Table 2 and the outflow properties were derived on the basis of this distance.

In Table 2, representative properties of bipolar outflows thought to be driven by massive protostars are tabulated. I have reported values as given by the authors without insisting that the data be analyzed in a uniform and systematic way. As a consequence, there are disagreements among different authors on some flow properties perhaps at the factor of two level. Many of the sources have been observed by numerous observers with different techniques. In these cases, either the most complete set of published values or the latest values are generally given. Several sources, known to have outflows, are included for which no outflow properties are measured (eg. G10.62 and G34.26). The data given in Table 2 are from single dish observations which do not suffer from the "missing flux" problem that plagues interferometers and therefore provides more reliable global properties of the outflows such as mass, extent, and energetics but gives little information

Table 1
Massive Outflows

Source	RA(1950)	DEC(1950)	D kpc	L_{HII} $L_\odot$	L_{IR} $L_\odot$	Refs	Notes
W3(IRS5)	02 21 53.1	61 52 22	2.3		2.00x10^5	1	1
GL 490	03 23 39.2	58 36 36	0.9		1.7-2.4x10^3	1,2	
Orion IRC2	05 32 46	-05 24 00	0.5	>1.00x10^4	2.10x10^5	2,16	5
G173.58+2.45	05 36 06.2	35 39 06	1.8	3.00x10^3	1.80x10^3	3,5,14	
G192.16-3.82	05 55 20.0	16 31 44	2.0	3.00x10^3	3.26x10^3	3,5,14	
MonR2(IRS1)	06 05 20.0	-06 22 39	1.0	4.00x10^4	5.00x10^4	4,5,6	
G240.31+0.07	07 42 45.1	-24 00 24	6.4	1.26x10^4	5.01x10^4	7	
NGC6334 I	17 17 32.3	-35 44 04	1.7	3.00x10^4	8.00x10^4	8	
G5.89-0.39	17 57 26.8	-24 03 55	3.0	1.20x10^5	3.00x10^5	4,5	
G9.62+0.19 F	18 03 16.09	-20 31 59.7	5.7			13	2
G10.62-0.38	18 07 30.7	-19 56 29	6.5	2.10x10^5	1.24x10^6	4,5	
G25.65+1.05	18 31 40.1	06 02 06	2.8	8.90x10^3	1.76x10^4	9,5	
G34.26+0.15	18 50 46.1	01 11 12	3.7	1.40x10^5	5.93x10^5	4,5	
G35.2N (IRS1)	18 59 14.1	01 09 03	2.5	9.10x10^4	1.23x10^5	4,5,14	
G45.07+0.13	19 11 00.4	10 45 43	8.3	1.40x10^4	1.42x10^6	4,5	
G45.12+0.13	19 11 06.2	10 48 25	8.3	5.80x10^5	1.66x10^6	4,5	
IRAS20126+4104	20 12 41.0	41 04 20.5	1.7	5.01x10^3	6.31x10^4	7,15	
G75.78+0.34NE	20 19 52.7	37 27 22	5.5	4.80x10^4		3,5	
GL 2591	20 27 35.8	40 10 14	2.0	2.00x10^4	9.00x10^4	1,5	
W75NBb	20 36 50.0	42 26 57	2.0	5.50x10^3	1.40x10^5	10,5	
DR21	20 37 14.4	42 08 55	3.0	4.00x10^5	~6x10^5	11,5	
G98.04+1.45	21 41 21.3	54 42 32	7.4	2.30x10^5	1.39x10^5	3,5,14	3

Table 1 (continued).

Source	RA(1950)	DEC(1950)	D kpc	L_{HII} $L_\odot$	L_{IR} $L_\odot$	Refs	Notes
S140 (IRS1)	22 17 41.2	63 03 45	0.9		0.5-9.0x10^4	1,2	1
Ceph A	22 54 19.0	61 45 47	0.7	3.98x10^3	1.58x10^4	7	
NGC7538(IRS9)	23 11 52.8	61 10 59	2.7		4.00x10^4	12	1
G111.25-0.77	23 13 57.9	59 39 00	3.5	2.00x10^4	9.80x10^3	3,5,14	4
IRAS23385+6053	23 38 31.4	60 53 50	4.9		1.60x10^4	17	6

References

1. Choi (*et al.)(1993)*
2. Cabrit & Bertout (1992)
3. Shepherd & Churchwell (1996)
4. Wood & Churchwell (1989)
5. Panagia (1973)
6. Thronson *et al.* (1980)
7. MacLeod *et al.* (1998)
8. Bachiller & Cernicharo (1990)
9. Shepherd & Churchwell (1995)
10. Hunter *et al.* (1994)
11. Garden & Carlstrom (1992)
12. Mitchell & Nasegawa (1991)
13. Hofner *et al.* (1995)
14. Shepherd (private communication)
15. Cesaroni *et al.* (1997)
16. Menten & Reid (1995)
17. Molinari *et al.* (1998)

Notes

1. The IR source does not coincide with a detected HII region.
2. No cm emission detected, mm emission is from warm dust. FIR emission is confused.
3. Two UC HII regions are present, neither of which is likely powering the outflow.
4. There may be multiple outflows toward this UC HII region.
5. The outflow source is not the radio source, as its luminosity is much too small.
6. No cm emission detected, mm emission is probably due to dust.

Table 2
Typical Properties of Massive Bipolar Outflows

Source	R_f pc	τ_d 10^4 yr	M_f $M_\odot$	$\dot{M}_f$ $M_\odot$ yr^{-1}	P_f $M_\odot$ km s^{-1}	E_f 10^{45} ergs	L_f $L_\odot$	Refs.	Notes
W3 (IRS5)		0.3	$\sim$8	$4.8\text{x}10^{-5}$	110	16		1	1
GL 490	1.2	1.8	15.4	$8.6\text{x}10^{-4}$	493	158	19	2.1	2
Orion IRC2	0.1	0.075	8.2	$1.1\text{x}10^{-2}$	533	346	1000	2	3
G173.58+2.45	0.6	5.3	32	$6.0\text{x}10^{-4}$	170	9.4	1.4	3	4
G192.16-3.82	2	27	58	$2.2\text{x}10^{-4}$	210	9.4	0.2	3	4
MonR2 (IRS1)	$\geq$3.2	15	202	$1.3\text{x}10^{-3}$	$\sim$2000	290	16	4,5,6,7	
G240.31+0.07	0.76	2.3	8.3	$3.6\text{x}10^{-4}$	93	11	3.9	8	7
NGC6334F	0.36	0.23	>2.3	$1.0\text{X}10^{-3}$	92	43	170	9	
G5.89-0.39	0.1	0.3	77	$2.6\text{X}10^{-2}$	990	500	1300	10,11,1	5,2
G9.62-0.19F		0.8	$\sim$50					20	
G10.62-0.38								11	6
G25.65+1.05	1.1	1.8	7.6	$4.2\text{x}10^{-4}$	136	27	12.4	8	7
G34.26+0.15								11	6
G35.2N (IRS1)	1.4	4.6	73	$1.6\text{x}10^{-3}$	1100	164	51	2	
G45.07+0.13	0.3	3.2	50	$1.4\text{x}10^{-3}$	631	36	$\sim$11	12	
G45.12+0.13	1.8	20	$\sim$4800	$\geq1.3\text{x}10^{-3}$	$\sim$31000	5600	10-100	12	8
IRAS20126+4104	0.3	0.58	>90-310	$1.6\text{x}10^{-2}$	540		80	13	
G75.78+0.34NE	0.8	3	72	$2.4\text{x}10^{-3}$	970	130	36	3	
GL 2591		0.2	33	$6.8\text{x}10^{-5}$	269	23		1	1
W75N	0.7	$\geq$4.4	48	$1.2\text{x}10^{-3}$	$\sim$700	110	22	14,15	
DR21	$\sim$2.2		>3000			>2000		16,17,18	9
G98.04+1.45	1.2	9.1	40	$4.4\text{x}10^{-4}$	240	15	1.4	3	
S140 (IRS1)	1.1	11	24.4	$9.4\text{x}10^{-4}$	488	98	8.4	2,1	
Ceph A		0.2	$\sim$8	$2.8\text{x}10^{-5}$	86	10		1	1

Table 2 (continued)

Source	R_f pc	τ_d 10^4 yr	M_f $M_\odot$	$\dot{M}_f$ $M_\odot$ yr^{-1}	P_f $M_\odot$ km s^{-1}	E_f 10^{45} ergs	L_f $L_\odot$	Refs.	Notes
NGC7538 (IRS9)	0.97	~1.6	51	4.2×10^{-3}	490	100	790	19	
G111.25-0.77	0.6	3.7	16	4.3×10^{-4}	110	8.4	1.8	3	
IRAS23385+6053	>0.01	<0.73	11-20	$>1.5 \times 10^{-3}$	≥67	>4.7	>5.4	21	

References

1. Choi *et al.* (1993)
2. Cabrit & Bertout (1992)
3. SC96
4. Wolf, Lada, & Bally (1990)
5. Loren (1981)
6. Tafalla *et al.*(1997)
7. Meyers-Rice & Lada (1991)
8. SC95
9. Bachiller & Cernicharo (1990)
10. Acord *et al.* (1997)
11. Cesaroni *et al.* (1991)
12. Hunter *et al.* (1997)
13. Cesaroni *et al.* (1997)
14. Hunter *et al.* (1994)
15. Fischer *et al.* (1985)
16. Garden *et al.* (1991a)
17. Garden *et al.* (1991b)
18. Garden & Carstrom (1992)
19. Mitchell & Hasegawa (1991)
20. Hofner *et al.* (1995)
21. Molinari *et al.* (1998)

Notes

1. The mass and other reported flow properties assume the mass is swept-up ISM.
2. Ref. 2 only mapped the inner part of the outflows: they find lower values than other observers.
3. Many observers have studied this source; ref 2 values are reported here.
4. HPBW≈60".
5. Tabulated values are from ref 10, see note 2 above.
6. Images are shown but no outflow properties were given.
7. Optical depth unity was assumed.
8. Values from ^{12}CO are reported rather than those from ^{13}CO.
9. At least 2 outflows and probably more are present.

on multiplicity, detailed morphologies, and velocity distributions. The headings in Table 2 are, from left to right: the HII region or IR source toward which the outflow is observed, the projected separation of the outflow lobes R_f, the dynamical time scale of the outflow $\tau_d = R_f/2v_f$, the total mass in the outflow M_f in solar masses, the rate of mass outflow $\dot{M}_f$, the outflow momentum P_f, the momentum supply rate or force of the outflow F_f, the total energy of the outflow E_f, and the mechanical luminosity of the outflow L_f in solar luminosities.

Aside from the usefulness of assembling the list of currently known massive outflows and their properties in one place, the main reason for assembling Table 2 was to provide an overview of massive outflow properties. These outflows are thought to be driven by massive protostars as implied by Fig. 13 below and the fact that massive outflows only occur in MSF regions (Table 2). Single dish spatial resolutions are not good enough to identify the source of the outflow with a particular star or protostar. Identification of the driving source is exacerabated by the fact that massive star formtion occurs in distant (typically d > 1 kpc), dense stellar clusters. This has been demonstrated by direct near infrared imaging of MSF regions (McCaughrean 1993; Mc Caughrean and Stauffer 1994; Aspin and Walther 1990; and others); by optical imaging of evolved HII regions which contain star clusters; and, indirectly by Kurtz, Churchwell, & Wood (1994) who showed that UC HII regions have 100 μm-to-2 cm flux density ratios well in excess of those produced by single stars of the same luminosity. In all cases where IR imaging has been carried out, a dense cluster of stars or protostars have been found to be associated with the UC HII region toward which outflows have been observed. Only radio interferometry in combination with high spatial resolution NIR imaging can isolate the sources of bipolar molecular outflows. In a few cases it appears that an outflow may be driven by the star responsible for ionizing a UC HII region, but outflows are often offset from the nearby UC HII region and probably driven by an even younger star than the ionizing star of the UC HII region. A consequence of large distances and crowded star fields is that the ionizing star of only one UC HII region (the relatively lightly extincted nebula G29.96) has been identified (Watson *et al.* 1998) to the present time and no star has been unambiguously identified as the driving source for a massive outflow.

Interferometric studies of G45.12, G75.78, and NGC2024 by Hunter, Phillips, & Menten (1997); Shepherd, Churchwell, & Willner (1997); and Chernin (1996) have shown that these regions harbor two or more outflows when observed with high spatial resolution. We also know that multiple outflows are present in DR21, even from single dish observations. The mass of each of the outflows (with the exception of the one toward NGC2024) is still quite large (10s to 100s $M_\odot$). The interferometric images have also shown that massive outflows do not appear to be well collimated. The Orion IRC2 outflow, traced by high resolution shocked H_2 emission (Allen & Burton 1993), is shown in Figure 12. This outflow is certainly not well collimated nor is it a smooth gaseous flow. It does not come to a point at its origin but rather appears to originate from a large surface area, most of which is well away from the central position of the outflow. Allen & Burton (1993) referred to it as an explosive event. The "fingers" of this outflow which reach out into the ambient interstellar medium defines a jagged interface not a smooth working surface. It has been suggested that the fingers might be jets from individual low-mass protostars at the center of this feature, although possible this explanation seems unlikely: one, because it would require many stars to have their jets aligned within about 45^0 of each other; two, NIR photometry does not implicate such stars along the waist of this bowtie feature (although this could be because of large 2μm optical depths); and three, the outflow looks like a coherent feature, not a montage of many separate features (althought this could be a resolution effect).

The outflows found in MSF regions have energetics, masses, and outflow rates much larger than those associated with low-mass star formation. This is illustrated quite clearly in Table 3 where the average outflow mass, force, and mechanical luminosity are tabulated from Lada (1985) for star formation regions with bolometric luminosity $L_{bol} > 10^3\ L_\odot$ versus those with L_{bol} <750 $L_\odot$. If the more recent data given in Table 2 had been used, the mean outflow mass and luminosity from MSF regions would be >130 $M_\odot$ and >180 $L_\odot$, respectively. The mean properties of low-mass outflows do not seem to have changed significantly excluding the discovery of much

TABLE 3. Comparison of Mean Outflow Properties

Selected Outflow Parameter	$L_{bol} > 10^3\ L_\odot$ Average	$L_{bol} < 750\ L_\odot$ Average
M_f ($M_\odot$)	44	1.8
F_f ($10^{-3}\ M_\odot$ km s^{-1} yr^{-1}	8.3	0.8
L_f ($L_\odot$	8	1.1

larger outflow radii. Thus, MSF regions have outflows at least a factor of ten more massive and more luminous than those from low-mass stars. SC96 have shown that the mass outflow rate $\dot{M}_f$ is a continuously increasing function of stellar bolometric luminosity over the range 1 to 10^6 $L_\odot$ as shown in Fig. 13. The solid curve is a quadratic least squares fit to the

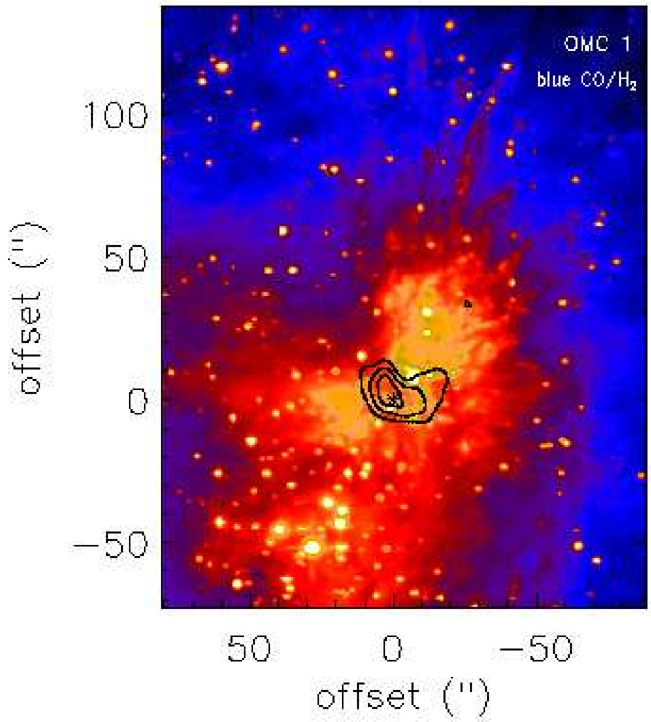

Figure 12. The Orion IRC2 outflow as delineated by shocked H_2 (in grey scale) from Allen & Burton (1993) with CO(1-0) emission contours superimposed from Chernin & Wright (1996).

data. A linear least squares fit to the data implies that

$$\dot{M}_f \approx L_{bol}^{0.7} \propto M_*^{2.1} \tag{1}$$

The dependence on stellar mass assumes a mass-luminosity relation (M-L) $L \propto M^3$ (appropriate for the upper end of the M-L relation). The importance of the tight relation between $\dot{\mathrm{M}}_f$ and L_{bol} is that one can measure $\dot{\mathrm{M}}_f$ relatively easily from which it is possible to infer the luminosity of the driving source to relatively high accuracy, even in the absence of radio continuum or IR fluxes. Further, the product of $\dot{\mathrm{M}}_f$ with the stellar luminosity function Φ(M) (Allen 1972), when plotted against L_{bol} indicates that A-F protostars are the major contributors to mass outflow during star formation. In principle, it is only legitimate to make such a plot for outflow sources of the same age; however from Table 2, we see that most massive outflows have ages within a factor of 10 of each other.

SC96 also showed that within a given luminosity range, the outflow mass increases with age as one would expect and that flows driven by luminous

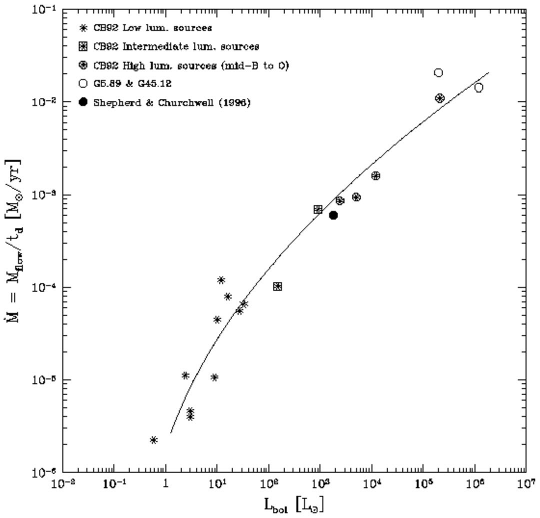

Figure 13. The mass outflow rate $\dot{M}_f$ versus the bolometric luminosity L_{bol} inferred from integrated far infrared flux densities. This figure is a compilation of data from several sources as described in SC96. A tight and continuous relationship between $\dot{M}_f$ and L_{bol} exists from 1 to 10^6 solar luminosities.

stars are substantially more massive than those driven by lower luminosity stars of the same age. For example, the Orion IRC2 outflow has almost 10^3 times more mass than that of L1448C even though the L1448C outflow is about 10 times older than the Orion IRC2 outflow.

8.3. ISSUES RAISED BY MASSIVE OUTFLOWS

The large masses and energetics associated with young molecular outflows from forming massive stars raise some very puzzeling questions. Among these are: How can several tens of solar masses of gas be accelerated to supersonic speeds on timescales of $\sim 10^4$ years and remain cold and neutral?; What supplies the momentum to the outflows?; What is the origin of the mass in the outflows?; What is the driving mechanism of the outflows?; and, Why is there no clear evidence of the outflow in the morphologies of UC HII regions? That is, why does one not see obvious disruptions in the shells of cometary or shell-like HII regions where the outflow has broken through the ionized shell. A good example of this is the shell-like UC HII region G5.89 with which a massive and very energetic molecular outflow has been identified (Harvey & Forveille 1988; Acord, Walmsley, & Churchwell 1997). This HII region is shown in Figure 14. Although there is a low intensity extension of the nebula in the SE-NW direction, there is no evidence that the dense, inner, bright shell has been disrupted by a bipolar outflow.

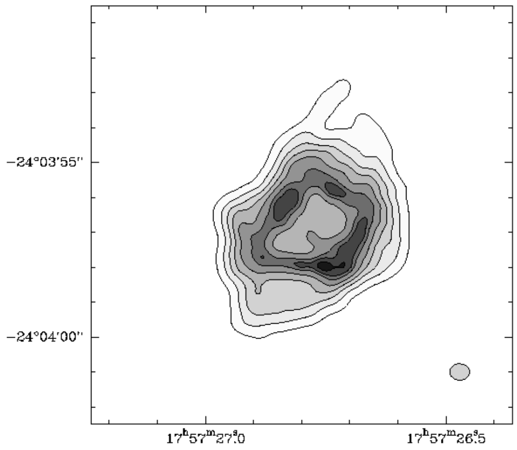

Figure 14. A 3.6 cm VLA image of the shell-like UC HII region G5.89-0.39 from ACW98. The synthesized beam (HPBW=0.57"x0.47") is shown in the lower right corner. The coordinates are RA and Dec (1950) and the coutours are similar to those given in Fig. 1 of ACW98.

A possibility is that the outflow does not originate from the ionizing star of the HII region but from another massive star at an earlier evolutionary age which has not been able to form a detectable HII region yet because of rapid accretion of matter onto the star. Another is orientation of the outflow relative to the line of sight. If the outflow were aligned close to the line of sight, one would not necessarily see evidence of this in the morphology of the HII shell. It is unlikely that this explanation holds for all shell-like or cometary nebulae, however. In the following section, I will consider possible origins of the large outflow masses and discuss their implications.

8.4. ORIGIN OF THE MASS IN MASSIVE OUTFLOWS

Churchwell (1997b) noticed that outflow masses are often more massive than the mass of the central protostar believed to be responsible for driving the outflow (inferred from Fig. 13 in conjunction with the mass-luminosity relation). Possible mechanisms to achieve such massive outflows were discussed by Churchwell (1997b) which I will review here with some updating and illustrations. Four possible mechanisms are: accumulated stellar winds; entrained interstellar medium in bipolar jets; swept-up interstellar medium; and, in-falling matter deflected into bipolar outflows.

8.4.1. *Accumulated Stellar Winds*

The idea is illustrated in Figure 15 where a high mass flux, bipolar stellar wind is blown away from the protostar in directions perpendicular to the

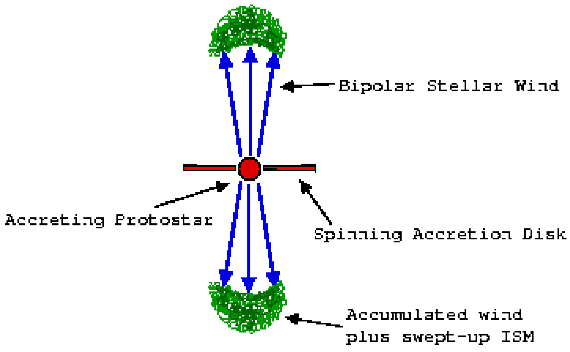

Figure 15. A schematic illustrating accumulation of stellar wind material from a polar wind. A segment of the accretion disk is shown edge-on.

accretion disk. The accumulated wind material plus whatever ISM has been accelerated by the wind is indicated at the ends of the outflows.

The winds from O and B stars are radiation driven (Abbott 1985; Lamers & Groenewegen 1990; Pauldrach *et al.* 1990; Castor 1993). For stellar winds to supply an outflow of 50 $M_{\odot}$ over a typical period of 10^4 yr, the average mass loss rate would have to be $\sim 5x10^{-3} M_{\odot}$ yr^{-1}. This is about two orders of magnitude greater than the highest mass loss rate observed toward O-stars and WR stars. A mass loss rate of this magnitude, if it is radiation driven, cannot be greater than $(L_*/c)/v_\infty$ where L_* is the luminosity of the star, c is the speed of light, and v_∞ is the wind terminal velocity. This requires that the wind terminal velocities must be in the range 0.4 to 4 km s^{-1} for $L_* = 10^{5-6}\ L_{\odot}$. Such velocities are several times lower than observed molecular outflow velocities.

Mass accumulations could be greater if the dynamical lifetimes (determined from the outflow lobe separation divided by the outflow speed) under-estimates the actual ages possibly because of confinement by ambient pressure. Inclination of the outflow axis to the line of sight foreshortens the lobe separation and the flow velocity in the same way so τ_d is independent of inclination effects. The typical pressure applied by massive outflows is 4-5 orders of magnitude greater than that of the ambient ISM. It therefore seems unlikely that the ambient pressure can significantly increase the lifetime beyond that implied by the dynamical age. The effective radiative momentum can be increased, and therefore mass-loss rates increased, if multiple scattering is important. Lucy & Abbott (1993) and Gayley, Owocki, & Cranmer (1995) have shown that multiple scattering can increase the mass-loss rate by as much as a factor of 10 in extreme cases (factors ≤ 3 are more typical), but only in a spherically symmetric geometry and only

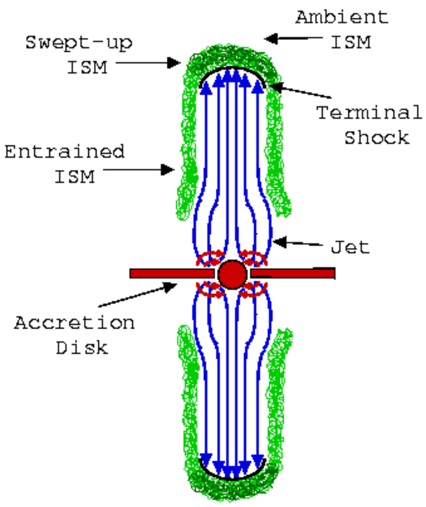

Figure 16. A schematic of entrained plus swept-up interstellar matter along the interface of a bipolar jet with the ambient interstellar medium. A segment of the accretion disk is shown edge-on with arrows showing matter going from the disk to the star and some arrows indicating a flow of matter into the jet from both the star and the inner accretion disk. It is not known where the jets actually originate (i.e. disk, star, or both).

when comoving opacities are large. In a bipolar outlfow, multiple scattering is unlikely to be important because of scattering losses perpendicular to the flow axis. Thus, neither increases in τ_d by ambient pressure nor multiple scattering appears to be capable of increasing the accumulated outflow masses by large enough factors to account for the observed values. The fact that $\dot{M}_f \propto L_{bol}^{0.7}$ (Fig. 13) also indicates that a wind cannot drive the outflows since radiatively driven winds have $\dot{\mathrm{M}}_w \propto L_{bol}^{1.7}$. The outflow masses are unlikey to be the result of accumulated stellar winds plus swept-up ISM, because they do not have enough radiative momentum.

8.4.2. *Entrained ISM in Stellar Bipolar Jets*

We consider here a highly collimated, high speed, bipolar jet ejected along the spin axis of a rapidly accreting, massive protostar. It is not known whether the jets originate from the inner disk, the protostar, or both. In this scenerio, a mixing layer at the interface of the jet walls with the ambient ISM entrains matter and accelerates the entrained matter in the direction of the jet flow. Also, some ISM will be accelerated ("swept-up") at the leading shock fronts ("working surfaces") of the jets. This scenerio is sketched in Figure 16.

The issue here is how much ISM can be entrained in a bipolar stellar jet. The mass entrainment rate per unit area is

$$\dot{M}_e = \epsilon \rho_o c_o \tag{2}$$

(Cantó and Raga 1991) where ϵ is the entrainment efficiency, ρ_o is the ambient ISM density, and c_o is the speed of sound in the ambient ISM. For T = 20-50 K and $N_{H_2} \approx 10^5$ cm^{-3},

$$\dot{M}_e = \epsilon(0.9 - 1.4)x10^{-14} gm\ cm^{-2}\ s^{-1} \tag{3}$$

If we take the central flow in G75.78NE as an example (see Shepherd, Churchwell, & Willner 1997), we have a lobe separation of 0.69 pc and an age of $3.7x10^4$ yr. To estimate its area, an approximate cone shape is assumed. For a flow mach number in the range 10-20, the jet opening angle is expected to be $\theta = 2/\sigma \approx 0.04$ rad=2.3^0 from experimental results for a "mixing layer limited" entrainment regime (see fig. 2 in Cantó and Raga 1991). In the above, σ is the "spreading parameter" which is inversely proportionaly to the opening angle. This gives a total surface area (both lobes) of about $1.5x10^{35}$ cm^2 and an entrained mass

$$M_f = R_e A_{flow} \tau_d \approx \epsilon(0.8 - 1.2) M_\odot \tag{4}$$

where A_{flow} is the area of the turbulent mixing layer of the jet and τ_d is the dynamical lifetime of the outflow. In the case of stellar jets with temperature $T_j \approx 10^4$ K and an ambient temperature $T_o < 100$ K, Cantó and Raga (1991) find that the "mixing layer limited" regime is appropriate and that the entrainment efficiency in this regime is $\epsilon < c_o/2c_j$ where c_o and c_j are the sound speed in the ambient medium and the jet, respectively. For the above conditions, $\epsilon < 0.1$ and the total mass of entrained ISM would be $M_f < 1M_\odot$. One could increase the entrained mass by assuming that the stellar mass loss occurs not as a narrow jet but as a flow of matter with much larger opening angles. For example, if $\theta = 30^0$, $M_f \approx \epsilon(13-20)M_\odot \leq 2M_\odot$. Thus, even in the large opening angle case, one can only entrain a few solar masses in outflows; certainly nothing like the several tens of solar masses observed.

Three caveats are in order here. One, the entrained mass is proportional to the third power of the lobe separttion. An under-estimate of this parameter would increase the estimated entrained mass. On average this effect would under-estimate the lobe separation by a factor of $\sqrt{2}$, which results in an average under-estimate of M_f by a factor of $\sim 35\%$, not enough to account for the observed masses. Two, this whole analysis depends on the entrainment efficiency ϵ being small relative to unity. The conclusion of Cantó and Raga (1991) that ϵ is small is based on experimental data and theoretical arguments. If, however, the experimental data are not applicable

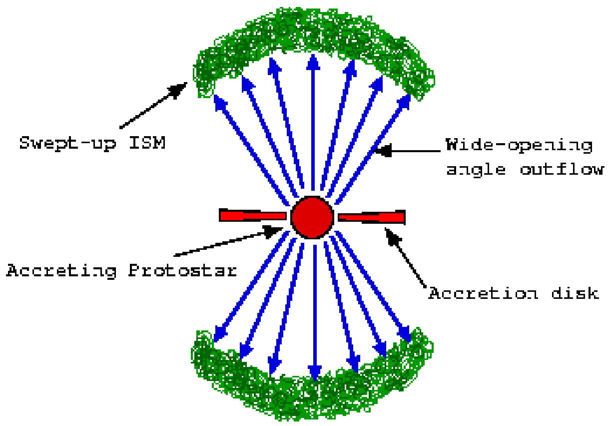

Figure 17. A schematic of swept-up interstellar matter due to a wide-angle outflow with a farily continuous terminal shock surface.

to the conditions in the ISM, then the entrained mass could be substantially greater. Three, there is clearly evidence for entrainment of ISM in low-mass outflows and one will surely find similar evidence in massive outflows when the data become precise enough to measure it. However, the masses involved in low-mass outflows are typically a small fraction of a solar mass. Such masses are easy to account for by entrainment. It is much more problematic to account for 10s to 100s of solar masses by entrainment if Cantó and Raga (1991) are correct. However, caution is in order because it is not absolutely clear that the experimental data on which their conclusions rest are applicable to the ISM.

8.4.3. *Swept-Up ISM*

It is also possible to accelerate a large mass of ambient ISM into motion along an outflow axis if: 1) the ISM density surrounding a forming star is large; 2) the opening angle of the outflow is large (i.e. has a large working surface); and, 3) the interface of the outflow lobe (working surface) with the ISM is a reasonably continuous surface. Under these conditions, the outflow lobes could act like pistons or snow plows which sweep-up ISM along their leading shock fronts rather than sweeping aside the ISM as narrow jets tend to do. This scenerio is sketched in Figure 17.

ISM densities are large toward MSF regions (Cesaroni *et al.* 1991; Churchwell, Walmsley, & Wood 1992; Cesaroni, Walmsley, & Churchwell 1992; Hofner *et al.* 1995; and others). Thus the main issues are whether the opening angles are systematically large for MSF and if the interfaces of the outflows with the ISM indeed form reasonably impervious surfaces or are

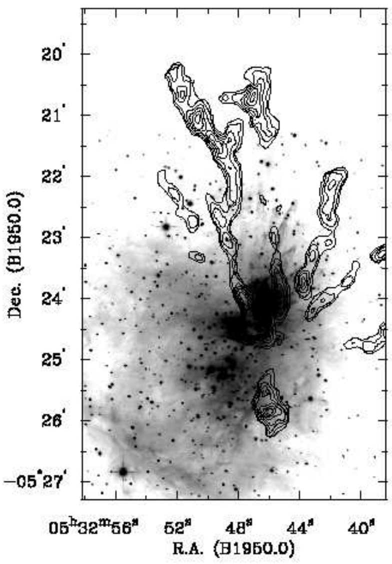

Figure 18. An overlay of NH_3 streamers (contours) from Wiseman and Ho (1998) onto the Allen & Burton (1993) shocked 2 μm H_2 outflow from Orion IRC2. This shows that all the streamers seem to be pointing toward the origin of the outflow and possibly shaped by the outflow flowing past the dense molecular clumps.

leaky pistons. None of the highest resolution data currently available (for G75.78, SCW97; G45.12, HPM97; and G192.16, SWSC98) indicate well collimated outflows. The opening angles of the outflows in all three of these regions seem to be several tens of degrees. Unfortunately, all these sources are $\geq$2 kpc away and the best millimeter interferometer resolutions do not match that of the best images toward Orion. Therefore, let us examine the Orion IRC2 shocked H_2 outflow (shown in Fig.13) as a possible prototype of an outflow from a massive protostar. First, it is clear that this outflow has a wide opening angle. Second, the interface with the ISM is not a smooth surface. In fact, Wiseman and Ho (1996;1998) have imaged NH_3(1,1 and 2,2) emission toward the outflow lobes of Orion IRC2 and find long filaments ($\geq$ 0.5 pc) of dense ammonia gas elongated parallel to the outflow axis (see Figure 18). These filaments are density enhancements as confirmed by $^{12}C^{18}O$ observations. They find a systematic change in velocity and temperature of the filaments with distance from the origin. These results are strongly suggestive that the elongation of the filaments is a result of the outflow stretching the dense molecular core condensations out into long filaments as the flow passes around the dense condensations and strike them on both sides from acute angles because of the wide opening angle of the outflow. It appears that rather than sweeping-up dense ISM components, the flow simply sweeps around them while stretching them out into long filaments aligned with the outflow axis and possibly superimposing a weak velocity gradient on the filaments. Thus, while the data suggest that there is a strong interaction of the outflow with the ISM, it is not a simple "snow plow" type interaction, but rather a very leaky snow plow that is not particularly effective at sweeping-up large masses of ISM. Much more work needs to be done before one can make a definitive statement on this issue. From the currently available data one can only get an impression of what might be happening, but there is certainly not enough data to be more quantitative or more certain about how effective wide-angle, massive outflows might be in sweeping-up large amounts of ISM.

8.4.4. *Accretion Driven Outflows*

Protostars, or more precisely their accretion disks, must shed angular momentum in order to accrete matter. The discovery of optical jets and radio bipolar molecular outflows associated with YSOs suggests that this is how they shed angular momentum and permit stars to form. The process by which accreting matter is diverted into outflows is not understood, especially for massive stars. Several models have been proposed (Pudritz 1988; Shu 1991, 1995; Shu *et al.* 1991, 1994; Fiege & Henriksen 1996a,b; Henriksen & Valls-Gabaud 1994; and others). In particular, Fiege & Henriksen (1996a,b) have developed protostellar bipolar outflow models in which infalling material is diverted into bipolar outflows due to high central pressures produced by radiative and/or dissipative heating. They find that these models are consistent with radio observations of molecular outflows. Tomisaka (1998) has developed a collapse-driven outflow model which achieves a mass outflow rate of $\sim$1/3 the accretion rate for a Class 0 low-mass protostar. Since entrainment and swept-up mass do not appear to be able to account for the very large observed outflow masses, it seems likely that deflection of infalling matter into bipolar outflows may be an important (perhaps primary) mechanism that feeds outflows of massive YSOs. This is illustrated in Figure 19.

Here, I will examine some of the consequences of this scenerio. First, it implies that massive YSOs must go through a very rapid accretion phase with a mass accretion rate $\dot{M}_{acc} > \dot{M}_f \sim 10^{-3}\ M_\odot\ \mathrm{yr}^{-1}$. $\dot{M}_{acc}$ must be larger than $\dot{M}_f$ since some of the accreting matter ultimately ends up on the central star. $\dot{\mathrm{M}}_{acc}$ also places restrictions on the density structure of the accreting matter. Since the infall cannot exceed the free-fall rate, if gravity is the only inward force, we have:

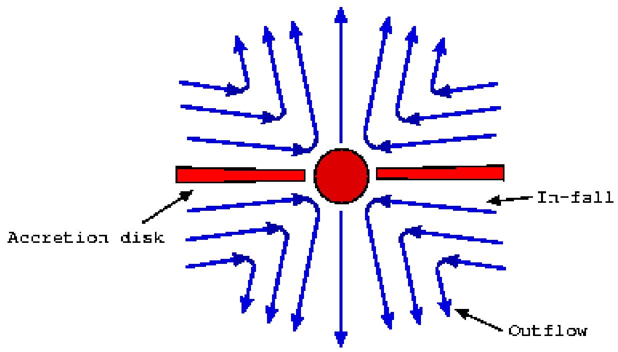

Figure 19. A schematic of in-falling matter diverted into a broad bipolar outflow. The physical mechanism for achieving this is not understood, although several models have been proposed (see text).

$$\rho(r) \geq \frac{\dot{M}_{acc} r^{-3/2}}{4\pi(2GM_r)^{1/2}} \tag{5}$$

where r is the distance from the central protostar and M_r is the mass (protostar, disk and core material) interior to r. This implies a very rapid increase in density toward accreting protostars, consistent with observations (Hofner *et al.* 1995; Bronfman, Nyman, and May 1996).

Second, the outflow plus stellar mass gives the minimum mass that a molecular cloud core must have to form a star of a given mass. For example, the central outflow in the G75.78NE region is apparently driven by an early B-star (M_* about 16 $M_\odot$) and it has an outflow mass of about 58 $M_\odot$. Thus the fraction of the infalling matter actually incorporated into the star is only about 15% and about 85% is deflected back outward into the outflow. In this sense, the efficiency of getting matter onto the central star is only about 15% and one concludes that a cloud core with a mass at least 6-7 times that of the final star is required to form the star. But we know that massive stars only form in clusters, so the initial cloud mass is probably $\geq$100 times that of the most massive star. This may also be part of the reason why massive stars are so rare; typical cloud cores generally do not achieve such large masses.

Third, accretion rates of 10^{-2} to 10^{-3} $M_\odot$ yr^{-1} will result in most of the stellar UV radiation being absorbed close to the central star, thus delaying the formation of a detectable UC HII region until after this phase of star formation. For example, a density greater than 10^8 cm^{-3} of in-falling matter toward an O5 star would result in a Strömgren sphere of radius $\leq$ 100 AU. This implies that the massive outflows observed to date are likely to be associated with YSOs that have not yet formed a detectable UC HII region. Those that appear to be driven by the central star of a UC HII region, such as G5.89, may either be relics of an earlier rapid accretion phase and no longer being driven or are misidentified. This has the further implication that detection of massive YSOs in their rapid accretion phase or earlier can only be achieved either via their molecular outflows or their thermal dust emission at FIR to mm wavelengths or high excitation molecular line probes, but not from radio free-free emission.

9. SUMMARY

A very brief review of the established properties of MSF regions was given, followed by an abbreviated description of six models that have been proposed to explain the morphologies, and/or ages, and/or dynamics of UC HII regions. The proposed models are: champagne flow or "blister models", in-fall models, photo-evaporating disk models, pressure confined UC HII regions, stellar wind supported bow shock models, and mass-loaded stellar winds. Each of these models predict different kinematics of the ionized gas and are therefore distinguishable, but relevant data are available for a very small number of nebulae. The angular expansion rate for one UC HII region, G5.89-0.39, has been measured (ACW98) to be 4 ± 1 mas yr^{-1}. Combined with an expansion rate of $\sim$35 km s^{-1}, estimated from radio recombination lines, a distance of $2^{+0.7}_{-0.4}$ kpc, independent of a galactic rotation model, was derived. The expansion age of this nebula is <1000 yr.

Because dust converts all radiation from a MSF region to far infrared (FIR) radiation, UC HII regions and their associated stellar cluster are among the most luminous objects in the Galaxy at FIR wavelenghts. Their emission generally peaks at $\sim$100 μm. Models of the spectral energy distributions of UC HII regions indicate that the dust resides in a shell surrounding the central star. A dust evacuated cavity of radius $\sim 10^{16}$ cm is required by the models to avoid too much near infrared emission. The average dust temperatures at the inner face of the dust shell are typically $\sim$300 K and they drop very rapidly in the inner 20% of the shell radius and then decrease more slowly in the remaining 80% of the dust shell. The 9.7 μm silicate feature is observed to be in absorption and is often very strong and broad.

Hot molecular cloud cores are heated by the ionizing stars of UC HII regions and their associated cluster members. These cores are dense, hot, compact, and dynamic. Typical properties are: densities $\sim 10^6$ cm^{-3}, temperatures $\sim$100-200 K, masses $\geq$1000 $M_\odot$, and diameters $\sim$0.5 pc. The densities and temperatures are not this high over the entire cloud core, just in the vicinity of the UC HII regions. Water and methanol masers are generally seen toward MSF regions. High resolution observations show that water maser spots are often found in linear structures. It is speculated that this may reflect the tendency of a collapsing cloud to form flattened disk-like structures which would produce linear structures when seen edge-on. This idea is also supported by the temperature profiles of hot cores which are well fit by disk-like models but poorly fit by spherical models.

Hard X-ray emission (up to 8 kev) has been detected toward one MFS region (W3). A model fit to the observed X-ray spectrum indicates a temperature $\geq 70x10^6$ K which is postulated to be associated with hot, stellar wind-shocked cavities immediately surrounding the ionizing stars of UC HII regions at the core of the W3 MSF complex. The 6.7 kev line of FeXXV has also been detected probably from the same gas responsible for the continuum X-ray emission. Presumably this is a general phenomenon associated with most if not all MSF regions, although only one has been observed to date.

During the past several years, massive molecular outflows have been detected toward MSF regions. The main conclusions regarding this phenomenon are as follows. Molecular outflows are found toward $\geq$50% of MSF regions. Typical outflow properties are: Mass outflow rates are in the range 10^{-2} to 10^{-4} $M_\odot$ yr^{-1} ($\dot{M}_f \propto L_{bol}^{0.7}$); outflow masses are in the range of 10s to 100s of solar masses; outflow ages are typically $\sim 10^4$ yr; collimation seems to be poor; opening angles seem to be wide (several 10s of degrees); and the energetics of massive outflows are $\geq$10 times those of low-mass outflows Massive outflows raise the interesting question of how several 10s of solar masses of material can be accelerated to supersonic speeds (relative to the ambient medium) over time scales $\leq 10^4$ yr and remain neutral (molecular) and cool. Possible origins of the mass in massive outflows associated with MSF were considered. It was shown that accumulated stellar winds cannot provide the momentum nor the mass observed. It does not appear possible to entrain 10s to 100s of solar masses of material into outflows if the Cantó and Raga (1991) analysis is correct. Also, the Orion IRC2 outflow seems to indicate that rather than sweeping-up large masses of ISM, outflows simply sweep by dense condensations of ISM in their paths. These arguments seem to favor the possibility that massive outflows may be accretion driven, but do not by any means constitute proof of such.

Questions raised in this review regarding molecular outflows will require much more observational underpinning to achieve further progress in their resolution. In particular, details of the outflow morphologies, their velocity structures, and their relationship to accretion disks need to be studied in much more detail.

ACKNOWLEDGEMENTS I thank Tim Drexler who helped me with the sketches for this review and Dorothy Churchwell who proofed the text for spelling and grammatical errors. I acknowledge partial support from NSF grant AST-9617686.

References

Abbott, D. C. 1985, in *Radio Stars*, eds. R. M. Hjellming & D. M. Gibson, Reidel, Dordrecht, p. 61

Acord, J. M., Churchwell, E., Wood, D. O. S. 1998, ApJ Lett., 475, L107 (ACW98)

Acord, J. M., Walmsley, C. M., Churchwell, E. 1997, Ap. J., 475, 693

Allen, C. W. 1973, *Astrophysical Quantities*, 3rd ed., The Athlone Press, Univ. London

Allen, D. A., Burton, M. G. 1993, Nature, 363, 54

Aspin, C., Walther, D. M. 1990, A&A, 235, 387

Bachiller, R., Cernicharo, J. 1990, A&A, 239, 276

Becker, R. H., White, R. L., Helfand, D. J., Zoonematkermani, S. 1994, ApJS, 91, 347

Bronfman, I., Nyman, L.-., May, J. 1996, A&A Suppl., 115,81

Cabrit, S., Bertout, C. 1992, A&A, 261, 274

Cant, J., Raga, A. C. 1991, Ap. J., 372, 646

Castor, J. I. 1993, in ASP. Conf. Proc. 35, *Massive Stars: Their Lives in the Interstellar Medium*, eds. J. P. Cassinelli & E. B. Churchwell, San Francisco, PSP, p.297

Cassinelli, J. P., Olson, G. L. 1979, ApJ, 229,304

Cesaroni, R., Churchwell, E., Hofner, P., Walmsley, C. M., Kurtz, S. 1994, Ast. Ap., 288, 903

Cesaroni, R., Felli, M., Walmsley, C. M., Olmi, L. 1997, A&A, 325, 725

Cesaroni, R., Hofner, P., Walmsley, C.M., Churchwell, E. 1998, Ast. Ap., 331, 709

Cesaroni, R., Walmsley, C. M., Churchwell, E. 1992, A&A, 256, 618

Cesaroni, R., Walmsley, C.M., Kmpe, C., Churchwell, E. 1991, A&A, 252, 278

Chernin, L. M. 1996, ApJ, 460,711

Chernin, L. M., Wright, M. C. H. 1996, 467, 676

Choi, M., Evans, N. J. II, Jaffe, D. T. 1993, Ap. J., 417, 624

Chini, R., Krgel, E., Kreysa, E. 1986, A&A, 167, 315

Churchwell, E. 1990, A&A Rev., 2, 79

Churchwell, E. 1991, in *The Physics of Star Formation and Early Stellar Evolution*, eds. C. J. Lada and N. D. Kylafis,Kluwer Acad. Pub., pp. 221-268

Churchwell, E. 1995, Ast. Sp. Sci., 224, 157

Churchwell, E. 1997a, in *Herbig-Haro Flows and the Birth of Low Mass Stars*, IAU Symp. No. 182, eds. B. Reipurth and C. Bertout, Kluwer Acad. Pub., Dordrecht, pp. 525-536

Churchwell, E. 1997b, ApJ Lett., 479, L59

Churchwell, E., Walmsley, C.M., Wood, D.O.S. 1992, A&A, 253, 541

Churchwell, E., Wolfire, M., Wood, D. O. S. 1990, ApJ, 354, 247 (CWW)

De Pree, C. G., Rodriguez, L. F., Goss, W. M. 1995, Rev. Mex. de Ast. y Astrofis.,31, No. 1, 39

De Pree, C. G., Goss, W. M., Gaum, R. A. 1998, ApJ, 500, 847

Dickel, H. R., Goss, W. M., Condon, G. R. 1996, ApJ, 460, 716

Downes, D., Genzel, R., Becklin, E. E., Wynn-Williams, C. G. 1981, Ap. J., 244, 869

Dyson, J. E. 1994, in *Lecture Notes in Physics*, Vol 431, ed. T. P. Ray and S. V. W. Beckwith, Berlin: Springer-Verlag, p93

Dyson, J. E., Williams, R. J. R., Redman, M. P. 1995, MNRAS, 277, 700

Erickson, N. R., Goldsmith, P. F., Snell, R. L., Berson, R. L., Huguenin, G. R., Ulich, B. L., Lada, C. J. 1982, Ap. J. Lett., 261, L103

Faison, M., Churchwell, E., Hofner, P., Hackwell, J., Lynch, D. K., Russell, R. W. 1998, ApJ, 500, 280

Fey, A. L., Gaume, R., Claussen, M. J., Vrba, F. J. 1995, ApJ, 453,308

Fiege, J. D., Henriksen, R. N. 1996a, MNRAS, 281, 1038

Fiege, J. D., Henriksen, R. N. 1996b, MNRAS, 281, 1055

Fischer, J., Sanders, D. B., Simon, M., Solomon, P. M. 1985, Ap. J., 293, 508
Forster, J. R., Caswell, J. L, Okamura, S. K., Hasegawa, T., Ishiguro, M. 1990, A&A, 231, 473
Garay, G., Lizano, S. , Gomez, Y. 1994, ApJ, 429, 268
Garden, R. P., Geballe, T. R., Gatley, I., Nadeau, D. 1991a, Ap. J., 366, 474
Garden, R. P., Hayashi, M, Gatley, I., Hasegawa, T. Kaifu, N. 1991b, Ap. J., 374, 540
Garden, R. P., Carlstrom, J. E. 1992, Ap. J., 392, 602
Gayley, K. G., Owocki, S. P., Cranmer, S. R. 1995, ApJ, 447, 296
Harvey, P. M., Forveille, T. 1988, A&A, 197, L19
Helfand, D. J., Zoonematkermani, S., Becker, R. H., White, R. L. 1992, ApJS, 80, 211
Henriksen, R. N., Valls-Gabaud, D. 1994, MNRAS, 266, 681
Ho, P. T. P., Haschick, A. D. 1986, ApJ, 304, 501
Hoare, M. G., Glencross, W. M., Roche, P. F., Clegg, R. E. S. 1988, in *Dust in the Universe*, eds. M. E. Bailey and D. A. Williams, Cambridge Univ. Press.
Hofner, P., Churchwell, E. 1996, A&A Suppl., 120, 283
Hofner, P., Churchwell, E. 1997, ApJ Lett, 486, L39 (HC97)
Hofner, P., Kurtz, S., Churchwell, E., Walmsley, C. M., Cesaroni, R. 1995, ApJ, 460, 359
Hollenbach, D., Johnstone, D., Shu, F. 1993, in *Massive Stars: Their Lives in the Interstellar Medium*, eds. J. P. Cassinelli and E. Churchwell, A. S. P. Conf. Series, 35, p26
Hollenbach, D., Johnstone, D., Lizano, S., Shu, F. 1994, ApJ, 428, 654
Hunter, T. R., Phillips, T. G., Menten, K. M. 1997, Ap. J., 478, 283 (HPM97)
Hunter, T. R., Taylor, G. B., Felli, M., Tofani, G. 1994, A&A, 284, 215
Keto, E. R., Ho, P. T. P., Haschick, A. D. 1987, ApJ, 318, 712
Keto, E. R., Ho, P. T. P., Haschick, A. D. 1988, ApJ, 324, 920
Keto, E. R., Ho, P. T. P., Reid, M. J. 1987, ApJ Lett, 323, L117
Koyama, K., Asaoka, I., Kuriyama, T., Tawara, Y. 1992, PASJ, 44, L255
Krgel, E., Mezger, P. G. 1975, A&A, 42, 441
Kurtz, S., Churchwell, E., Wood, D. O. S. 1994, ApJ Suppl, 91, 659
Kwan, J., Scoville, N. Z. 1976, Ap. J., 459, 638
Lada, C. J. 1985, ARA&A, 23, 267
Lamers, H. G. J. L. M., Groenewegen, M. A. T. 1990, in ASP. Conf. Proc. 7, *Properties of Hot Luminous Stars*, ed. C. D. Garmany, San Francisco, ASP, p 189.
Lee, H. M., Draine, B. T. 1985, ApJ, 290, 211
Leung, C. M. 1976, ApJ, 209, 75
Lizano, S., Cant, J., Garay, G., Hollenbach, D. 1996, ApJ, 468, 739
Loren, R. B. 1981, Ap. J., 249, 550
Lucy, L. B. 1982, ApJ, 255, 286
Lucy, L. B., Abbott, D. C. 1993, ApJ, 405, 738
Lumsden, S. L., Hoare, M. G. 1996, ApJ, 464, 272
MacLeod, G. C., Scalise, E. Jr., Saedt, S., Galt, J. A., Gaylard, M. J., 1998, AJ, in press
MacLow, M.-M., Van Buren, D., Wood, D. O. S., Churchwell, E. 1991, ApJ, 369, 395
Massi, M., Felli, M., Simon, M. 1985, A&A, 152, 387
Masson, C. R. 1986, ApJ, 302, L27
Masson, C. R. 1989, ApJ, 336, 294
Mc Caughrean, M. 1993, in *Massive Stars: Their Lives in the Interstellar Medium*, eds. J. P. Cassinelli and E. Churchwell, ASP Conf. Series, 35, 80
Mc Caughrean, M., Stauffer, J. R. 1994, AJ, 108, 1382
Menten, K. M., Reid, M. J. 1995, ApJ Lett., 445, L157
Meyers-Rice, B., Lada, C. J. 1991, Ap. J., 368, 445
Mitchell, G. F., Hasegawa, T. I. 1991, Ap. J., 371, L33
Molinari, S., Testi, L., Brand, J., Cesaroni, R., Palla, F. 1998, ApJ Lett., in press
Panagia, N. 1973, AJ, 78, 929
Pauldrach, A. W. A., Puls, J., Gabler, R., Gabler, A. 1990, in ASP. Conf. Proc. 7, *Properties of Hot Luminous Stars*, ed. C. D. Garmany, San Francisco, ASP, p. 171

Pudritz, R. E. 1988, in *Galactic and Extragalactic Star Formation*, eds. R. E. Pudritz and M. Fich, Kluwer Acad. Pub. Dordrecht, Netherlands, p. 135
Raymond, J. C., Smith, B. W. 1977, ApJS, 35, 419
Redman, M. P., Williams, R. J. R., Dyson, J. E. 1996, MNRAS, 280, 661
Reid, M. J., Haschick, A. D., Burke, B. F., Moran, J. M., Johnston, K. J., Swenson, G. W. Jr. 1981, ApJ, 239, 89
Roelfsema, P. R. *et al.* 1996, A&A Lett., 315, L289
Shepherd, D. S., Churchwell, E. 1995, Ap. J., 457, 267 (SC95)
Shepherd, D. S., Churchwell, E. 1996, Ap. J., 472, 225 (SC96)
Shepherd, D. S., Churchwell, E., Willner, D. J. 1997, ApJ, 482,355 (SCW97)
Shepherd, D. S., Watson, A. M., Sargent, A. I., Churchwell, E. 1998, ApJ, in press (SWSC98)
Shu, F. H. 1991, in *The Physics of Star Formation and Early Evolution*, eds. C. J. Lada and N. D. Kylafis, Kluwer Acad. Pub., Dordrecht, Netherlands, p. 365
Shu, F. H. 1995, Rev. Mex. A. A. (Ser. de Conf.), 1, 375
Shu, F. H., Najita, J., Ostricker, E., Wilkin, F., Ruden, S., Lizano, S. 1994, ApJ, 429, 781
Shu, F. H., Ruden, S. P., Lada, C. J., Lizano, S. 1991, ApJ, 370, 31
Tafalla, M., Bachiller, R., Wright, M. C. H., Welch, W. J. 1997, Ap. J., 474, 329
Thronson, H. A. Jr., Gatley, P. M., Sellgren, K., Werner, M. W. 1980, ApJ, 237, 66
Tielens, A. G. G. M., de Jong, T. 1979, A&A, 75, 326
Tomisaka, K. 1998, ApJ Lett., submitted
Tutukov, A. V., Shustov, B. M. 1981, Soviet Ast., 58, 109
Van Buren, D., Mac Low, M.-M., Wood, D. O. S., Churchwell, E. 1990, ApJ, 353, 570
Watson, A. M., Coil, A. L., Shepherd, D. S., Hofner, P., Churchwell, E. 1998, ApJ, in press
White, R. L., Becker, R. H., Helfand, D. J. 1991, ApJ, 371, 148
Williams, R. J. R., Dyson, J. E., Redman, M. P. 1996, MNRAS, 280, 667
Wiseman, J. J., Ho, P. T. P. 1996, Nature, 382, 139
Wiseman, J. J., Ho, P. T. P. 1998, ApJ, in press
Wolfire, M. G., Churchwel, E. 1994, ApJ, 427,889
Wood, D.O. S., Churchwell, E. 1989a, ApJ S, 69, 831(WC89a)
Wood, D. O.S., Churchwell, E. 1989b, ApJ, 340, 265
Wolf, G. A., Lada, C. J., Bally, J. 1990, A.J., 100, 1892
Wright, M. C. H., Plambeck, R. L., Vogel, S. N., Ho, P. T. P., Welch, W. J. 1983, Ap. J. Lett., 267, L41
Xie, T., Mundy, L. G., Vogel, S. N., Hofner, P. 1996, ApJ, 473, L131
Yamauchi, S., Koyama, K. 1993a, ApJ, 405, 268
Yamauchi, S., Koyama, K. 1993b, ApJ, 404, 620
York, H. W., Tenorio-Taglio, G., Bodenheimer, P. 1983, A&A, 127, 313
Zheng, X. W., Ho, P. T. P., Reid, M. J., Schneps, M. H. 1985, ApJ, 293, 522
Zoonematkermani, S., Helfand, D. J., Becker, R. H., White, R. L. 1990, ApJS, 74, 181
Zuckerman, B., Kuiper, T. B. H., Rodriguez Kuiper, E. N. 1976, Ap. J. Lett., 209, L137